Proceedings of HT-FED 2004
2004 ASME Heat Transfer/Fluids Engineering Summer Conference
Charlotte, North Carolina, USA, July 11-15, 2004

HT-FED2004-56633 DRAFT

MODELS AND EXPERIMENTS FOR LAMINAR NATURAL CONVECTION FROM HEATED BODIES IN ENCLOSURES

Peter M. Teertstra, M. Michael Yovanovich and J. Richard Culham
Microelectronics Heat Transfer Laboratory
Department of Mechanical Engineering
University of Waterloo
Waterloo, Ontario, Canada N2L 3G1
Email: pmt@mhtlab.uwaterloo.ca
mmyov@mhtlab.uwaterloo.ca
rix@mhtlab.uwaterloo.ca

ABSTRACT

A combined experimental and analytical study of natural convection heat transfer in the enclosure formed between an arbitrarily shaped, isothermal heated body and its arbitrarily shaped surrounding isothermal enclosure is presented. An experimental test program is conducted at atmospheric and reduced pressure conditions using a transient measurement technique for various enclosure configurations, including concentric cubes, cube-in-sphere, sphere-in-cube, and other geometries. Measurements are reported for a wide range of Rayleigh number, including the diffusive limit. An analytical modeling procedure is developed based on a composite solution of three asymptotic relationships, the conduction limit, the laminar boundary layer and transition flow convective limits. The composite model is in excellent agreement with the data, with an average RMS difference of 2 - 7 % for all enclosure configurations and test conditions.

NOMENCLATURE

A	area; (m^2)
b	semi-major axis, oblate spheroid; (m)
c	semi-minor axis, oblate spheroid; (m)
c_p	specific heat capacity; $(J/kg\,K)$
$\overline{C}_{cs}$	coefficient, Eq. (5)
d	diameter; (m)
$F(Pr)$	Prandtl number function, Eq. (18)
g	gravitational acceleration; (m/s^2)
$G_{\mathcal{L}}$	body gravity function, Eq. (19)
H	height; (m)
k	thermal conductivity; (W/mK)
k_e	effective conductivity, $\equiv kNu_{\mathcal{L}}/S^{\star}_{\mathcal{L}}$; (W/mK)
L, L'	effective length, equivalent cavity; (m)
$\mathcal{L}$	general characteristic length; (m)
n	combination parameter, Eq. (15)
m	mass; (kg)
$Nu_{\mathcal{L}}$	Nusselt number, $\equiv Q\mathcal{L}/\left(kA_i\Delta T\right)$
p	pressure; (Pa)
Pr	Prandtl number, $\equiv \nu/\alpha$
Q	total heat transfer rate; (W)
r	radius; (m)
R	thermal resistance, $\equiv (T_i - T_o)/Q$; $(^oC/W)$
$Ra_{\mathcal{L}}$	Rayleigh number, $\equiv g\beta\left(T_i - T_o\right)\mathcal{L}^3/\left(\nu\alpha\right)$
s	side length; (m)
$S^{\star}_{\mathcal{L}}$	dimensionless shape factor, $\equiv S\mathcal{L}/A_i$
T	temperature; (^oC)
T_b	bulk fluid temperature; (^oC)
V	enclosed volume; (m^3)
Z	compressibility factor

Greek Symbols

α	thermal diffusivity; (m^2/s)
β	thermal expansion coefficient; $(1/K)$
δ	gap thickness, $\equiv (d_o - d_i)/2$; (m)
ε	ellipticity, oblate spheroid $\equiv \sqrt{1-(c/b)^2}$
μ	dynamic viscosity; (Ns/m^2)
ν	kinematic viscosity; (m^2/s)
ρ	mass density; (kg/m^3)
τ	time constant, $\equiv m c_p R$; (s)

Subscripts

b	bulk fluid
bl	boundary layer flow
conv	convection
e	effective
ℓ	conduction losses
tr	transition flow
i	inner body
o	outer body
LB	lower bound
UB	upper bound
rad	radiation losses
tot	total

INTRODUCTION

Natural convection in the enclosure formed between a heated body and its surrounding cooled enclosure has been widely studied for a variety of applications, including nuclear reactor design, energy transmission and storage and solar energy. This enclosure configuration is of particular interest in the design of sealed equipment cabinets for microelectronic and telecommunications products for use in harsh or outdoor environments. The ability to model the overall heat transfer rate due to natural convection in these enclosures provides an easy-to-use design tool to quickly and accurately predict operating temperatures and perform parametric studies prior to more costly and time consuming prototype testing or numerical CFD simulations.

The problem of interest in the current study involves natural convection heat transfer from an isothermal heated, arbitrarily shaped body located at the center of an arbitrarily shaped, isothermal cooled enclosure, such that the body and enclosure form non-intersecting inner and outer boundaries on the fluid region, as shown in Fig. 1. The geometry of the enclosure is defined by three parameters that relate the inner and outer boundary geometries: relative boundary size, effective gap spacing and relative boundary shape. The relative boundary size is defined as the ratio of the outer to inner surface areas, A_o/A_i, which reduces to the diameter ratio, d_o/d_i, for the limiting case of the concentric spheres. The effective gap spacing is a dimensional parameter, closely related to the relative boundary size, which is important in conduction-dominated heat transfer. For the simple spherical

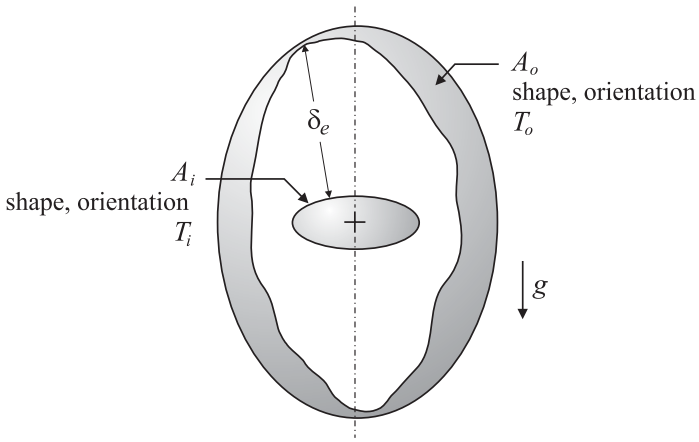

Figure 1. SCHEMATIC OF GENERAL 3D ENCLOSURE PROBLEM

enclosure it is defined as a uniform value $\delta = (d_o - d_i)/2$, while in more complex enclosures formed between different shaped boundaries, the gap spacing can vary significantly and an average effective value, δ_e, is required. A final parameter, the relative shape parameter, which relates variations in shape and orientation of the inner and outer boundaries with respect to the gravity vector, will be identified through the convection analysis.

The parameter of interest, the total heat transfer rate through the enclosed region, is calculated from the temperature gradient at the inner, heated boundary

$$Q = \iint_{A_i} -k \left.\frac{\partial T}{\partial \hat{n}}\right|_{A_i} dA_i \tag{1}$$

where $\hat{n}$ lies along the direction of an outward facing normal to the inner boundary. Non-dimensionalization using the general characteristic length $\mathcal{L}$ and the overall temperature difference, $T_i - T_o$, yields

$$Nu_{\mathcal{L}} = \frac{Q\,\mathcal{L}}{kA_i\,(T_i - T_o)} \tag{2}$$

The independent parameters are non-dimensionalized using the Rayleigh number, defined as

$$Ra_{\mathcal{L}} = \frac{g\beta\,(T_i - T_o)\,\mathcal{L}^3}{\nu\alpha} \tag{3}$$

where all properties are evaluated at the bulk fluid temperature, T_b.

For values of $Ra_{\mathcal{L}}$ less than some critical value, the heat transfer in the enclosure becomes conduction dominated and the

dimensionless heat transfer rate is equivalent to the dimensionless conduction shape factor

$$Nu_{\mathcal{L}} = S^{\star}_{\mathcal{L}} \tag{4}$$

Previous research on the topic of natural convection in enclosures with non-intersecting boundaries are divided into two categories: experimental and numerical CFD (computational fluid dynamics) studies, which often include correlations of the resulting data; and analytically based modeling and semi-empirical relationships.

Most experiments for natural convection are limited to the concentric spherical enclosure, with data often spanning only a few decades of Rayleigh number at the laminar boundary layer convection limit. Bishop et al. [1], [2], Mack and Hardee [3] and Scanlan et al. [4] all present data for air, water, and oil filled concentric spheres over a limited range of high Rayleigh number. McCoy et al. [5] and Powe et al. [6], [7] performed experimental measurements for the vertical circular cylinder with hemispherical ends in a spherical enclosure. Charmchi and Sparrow [8] and Sparrow and Charmchi [9] present a combined experimental and numerical study of concentric circular cylinders in both vertical and horizontal orientations. Powe and Warrington [10] report measured values for total heat transfer rate from an isothermal cube in a spherical enclosure for air, water, glycerine and oil, while Warrington and Powe [11] and Warrington et al. [12], [13] present experimental results for the sphere, the vertical circular cylinder with hemispherical ends and the cube in a cubical enclosure. In all of these cases, the available experimental data is limited to high Rayleigh number values indicative of laminar boundary layer convection.

Teertstra et al. [14] conducted an experimental test program for concentric spherical enclosure geometries $d_o/d_i = 1.5$, 2, 3, and 4.8, where the tests were performed in a reduced pressure environment. The resulting change in fluid density provided the means to obtain data over a wider range of Rayleigh number than the previous researchers, including the limiting case of conduction dominated heat transfer.

The remaining data available in the literature arises from numerical simulations, primarily for the limiting case of concentric spheres, including Mack and Hardee [3], Astill et al. [15], Caltagirone et al. [16], Singh and Chen [17], Ingham [18], Wright and Douglass [19], Fujii et al. [20], Garg [21], Chu and Lee [22] and Chiu and Chen [23]. There are currently no experimental data available in the literature for enclosures formed between bodies other than the concentric spheres that span the full range of Rayleigh number from laminar boundary layer convection to the conduction limit.

Two analytical expressions are available in the current literature for the enclosure problem; the model of Raithby and Hollands [24] and the empirical correlation of Warrington and Powe [11].

Raithby and Hollands [24] present an analytically based model for the limiting case of the concentric spherical enclosure, which is valid for the full range of Rayleigh number

$$\frac{k_e}{k} = \overline{C}_{cs}\,\frac{\delta^{1/4}}{d_i\,d_o}\,\frac{Ra_{\delta}^{\,1/4}}{{d_i}^{-7/5} + {d_o}^{-7/5}}\,, \quad \frac{k_e}{k} \geq 1 \tag{5}$$

where effective conductivity, k_e, is defined as the apparent value of thermal conductivity required for pure conduction through the enclosure to equal convection. Effective conductivity is related to the Nusselt number and dimensionless conduction shape factor by

$$\frac{k_e}{k} = \frac{Nu_{\mathcal{L}}}{S^{\star}_{\mathcal{L}}} \tag{6}$$

The parameter $\overline{C}_{cs}$ in Eq. (5) is a product of a Prandtl number function and a constant coefficient from an empirical fit of data of Bishop et al. [2] and Scanlan et al. [4] for $d_o/d_i = 2$.

In a subsequent publication, Raithby and Hollands [25] extend their model extended to include enclosures formed between different boundary shapes. The effective inner and outer diameter of an equivalent concentric spherical cavity are determined based on a preservation of the inner and outer body volume, as recommended by Warrington and Powe [11]. This approximation assumes inner and outer boundaries having similar shape and orientation as well as an aspect ratio close to unity; Raithby and Hollands provide no validation of this general model.

Following an extensive set of experimental measurements and numerical simulations for various combinations of spherical, cubical and cylindrical inner and outer body shapes, including Bishop et al. [1], [2], Mack and Hardee [3], Scanlan et al. [4], Weber et al. [26], Yin et al. [27], McCoy et al. [5], Powe et al. [6], [7] and Powe and Warrington [10], Warrington and Powe [11] propose the general correlation equation

$$Nu_b = 0.585\,Ra_b^{0.236}\left(\frac{\delta}{r_i}\right)^{0.236}\,, \quad \frac{\delta}{r_i} \geq 0.45 \tag{7}$$

where the scale length b is the boundary layer length of Lienhard [28], defined as the minimum distance traveled by the boundary layer on the inner body, assuming no flow separation. The effective gap spacing, δ, is defined as the distance between concentric spheres with volumes equivalent to the inner and outer bodies. This correlation is limited to high values of Rayleigh number and a narrow range of gap spacing

$$1.09 \leq \frac{d_o}{d_i} \leq 3.84\,, \qquad 4.6 \times 10^5 \leq Ra_b \leq 4 \times 10^{10}$$

with an average deviation from the data of 14.5% and a maximum difference of up to 90%.

The objective of the current study is to perform experimental tests and develop an analytically based model for the average heat transfer rate due to natural convection in the enclosure formed between an arbitrarily shaped, heated body and its arbitrarily shaped, cooled enclosure. The experiments will examine six different configurations, including the concentric cubes as well as enclosures formed between different boundary shapes, and will provide validation data for the analytical model. The model developed in this work will be valid for the full range of Rayleigh number, including the diffusive limit, and will be applicable to a wide range of inner and outer boundary shapes, orientations and relative sizes.

DESCRIPTION OF EXPERIMENTS

An experimental test program was carried out to measure natural convection heat transfer from an isothermal heated body concentrically located in an isothermal cooled enclosure. The main objective of the experiments was to provide validation data for the analytical models for enclosures with geometrically similar and dissimilar inner and outer boundary shapes.

The experimental apparatus and method used for these measurements is described in detail in Teertstra [29] and Teertstra et al. [14] for the limiting case of the concentric spherical enclosure. In order to satisfy the goals of the experimental test program, to perform measurements for a wide range of Rayleigh number including the conduction limit, the tests are performed in a reduced pressure environment, as described by Chamberlain et al. [30] and Hassani and Hollands [31]. If the air in the test chamber is treated as an ideal gas, a reduction in the absolute pressure results in a decrease in the mass density according to

$$\rho = \frac{p}{\mathcal{R} T_b Z} \tag{8}$$

where T_b is the bulk fluid temperature, $\mathcal{R}$ is the gas constant for air and Z is the compressibility coefficient. Substituting the relationship for ρ into Eq. (3) gives

$$Ra_{\mathcal{L}} = \frac{g\beta\,(T_i - T_o)\;\mathcal{L}^3 p^2 c_p}{\mathcal{R}^2 T_b^2 k \mu Z^2} \tag{9}$$

The fluid properties, β, c_p, k and μ, are assumed to be constant with respect to the pressure and are evaluated at the bulk temperature, T_b. An empirical correlation is used to calculate the compressibility for air, Z, as a function of both temperature and pressure.

The heat transfer through the enclosure due to convection, Q, is determined from an energy balance on the inner boundary

$$Q = Q_{\text{tot}} - Q_{\text{rad}} - Q_\ell \tag{10}$$

where Q_{rad} is the net radiative heat transfer, determined from an empirical correlation of high-vacuum, radiation test data, and Q_ℓ are the accumulated conduction losses through the wires and mounting structure. Q_{tot}, the total heat transfer rate due to all modes is measured using the transient test method of Hollands [32]. In the transient test procedure the inner body is heated to some specified initial temperature while the enclosure temperature remains constant throughout the test. When the prescribed temperature difference is established the power to the heater in the body is turned off and the transient response of the inner body is monitored. The total heat transfer rate is calculated based on these transient data

$$Q_{\text{tot}} = -mc_p \frac{dT_i}{dt} \tag{11}$$

where the heat capacity of the inner body, mc_p, is determined empirically in a previous test. The time derivative is approximated over distinct time intervals using a linear, least squares analysis of the temperature versus time data.

The use of the transient test method for steady state convection measurements in the enclosure is validated by Teertstra et al. [14] for the concentric spherical enclosure by comparing the time constants for the inner body with the enclosed air layer. The time constant is defined as

$$\tau = mc_p R \tag{12}$$

where R is the film resistance at the boundary. For the worst case of a small inner body in the enclosure, the ratio of the time constants for the inner body, τ_i and the fluid, τ_b, is

$$\frac{\tau_i}{\tau_b} \approx 19 \frac{R_i}{R_o} \tag{13}$$

Assuming that the convective resistances at the inner and outer boundaries are similar, $R_i \approx R_o$, it is obvious that, due to its much larger time constant, the cooling rate of the inner body controls the heat transfer process and a "quasi-steady" condition holds for the enclosed fluid region.

Experimental Apparatus

Two different surrounding enclosure geometries were examined in this work; the spherical and the cubical enclosure. Based on criteria described by Teertstra et al. [14], including limits on

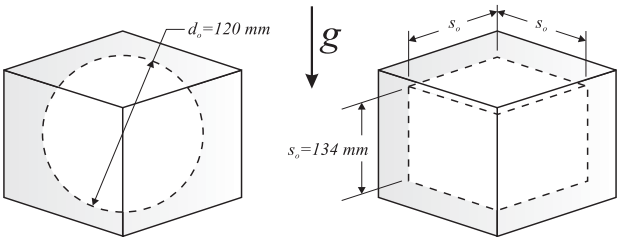

Figure 2. SCHEMATIC OF ENCLOSURE GEOMETRIES

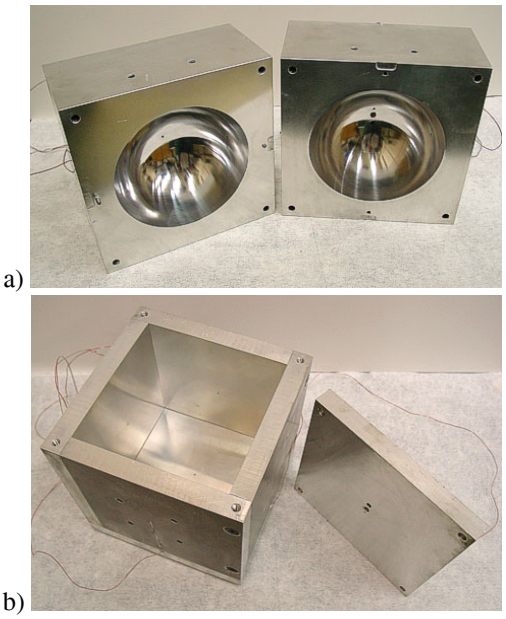

Figure 3. ENCLOSURES USED IN EXPERIMENTAL TESTS: a) SPHERICAL ENCLOSURE; b) CUBICAL ENCLOSURE

the space available in the vacuum chamber and rarefaction considerations at reduced pressure conditions, dimensions of the two enclosures were selected as shown in Fig. 2.

The enclosures were constructed using Al 6061 due to its high relative value of thermal conductivity. The spherical enclosure was constructed using two solid blocks with hemispherical cavities machined into one side, as shown in Fig. 3 a). The cubical enclosure was constructed using flat plate material joined at the edges using cap screws, as shown in Fig. 3 b). In both cases the inner surfaces of the enclosures were polished to minimize radiation heat transfer.

A series of inner bodies were used in the course of the measurements, including four different sized spheres and cubes as well as a circular cylinder, a cuboid and an oblate spheroid. All bodies were machined from Al 6061 and polished to minimize radiation heat transfer. Figure 4 presents the geometry and dimensions of each of the inner bodies.

Each inner test body was suspended at the center of the enclosure using a threaded phenolic rod turned into tapped holes in the enclosure and the body, as shown in Fig. 5. All temperature measurements were performed using T-type copper constantan thermocouples glued in shallow, small diameter holes drilled at the surface using aluminum-filled epoxy. For the inner body, two small diameter 36 AWG $(0.127mm)$ thermocouples were used to minimize conduction losses, while the enclosure used six thermocouples arranged at the top, bottom and evenly distributed about the midplane. All thermocouple measurements were based on an external reference junction that was maintained at 0 ± 0.1^oC by an ice point cell.

The inner bodies were heated using embedded cartridge resistance heaters, while the outer surfaces of the enclosures were

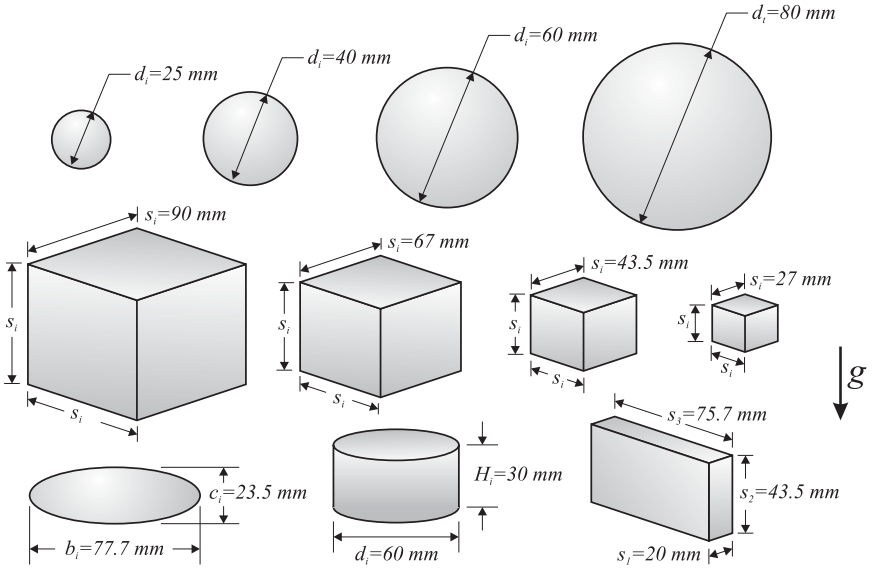

Figure 4. SCHEMATIC OF INNER BODY GEOMETRIES

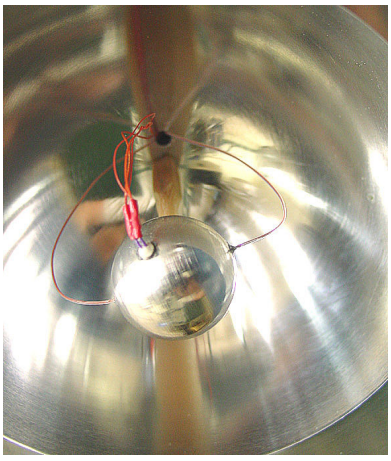

Figure 5. DETAIL OF INNER BODY MOUNTED IN ENCLOSURE

maintained at a constant temperature using liquid cooled cold plates. Heat was removed from the system via a glycol-water mixture circulated through the cold plates by a constant temperature bath. Figure 6 shows the assembled test apparatus, including all electrical, instrumentation and coolant connections, in the vacuum chamber.

Data acquisition and control of the experiment was performed using a Keithley 2700 data acquisition system and a Windows-based PC computer running Labview v.5.1 software. Absolute pressure in the test chamber was measured by a high accuracy vacuum gauge suitable for readings in the range 0.001 - 1 atm with an accuracy of $\pm$ 1.4×10^{-4} atm. A full uncertainty analysis of all measurement equipment and procedures is presented by Teertstra [29].

Experimental Procedure and Results

In order to provide data for model validation of a wide variety of enclosure configurations, various combinations of body and enclosure shapes were tested, including enclosures with similar shapes, such as the concentric cubes, and enclosures with different inner and outer boundary shapes, including the cube-in-sphere, sphere-in-cube, circular cylinder and cuboid in the cube, and oblate spheroid in the sphere. Figure 7 shows all the enclosure configurations examined in the experimental test program, with relative inner to outer boundary size expressed based on the ratio of the primary body dimensions; diameter, d, for the sphere and side length, s, for the cube.

Once the test body and enclosure are installed in the vacuum chamber, the test method for the natural convection measurements is as follows:

1. Seal the vacuum chamber and start both the first stage mechanical pump and the second stage diffusion pump to establish high vacuum conditions
2. Measure transient temperatures during heating test to determine an empirical heat capacity value for the inner body

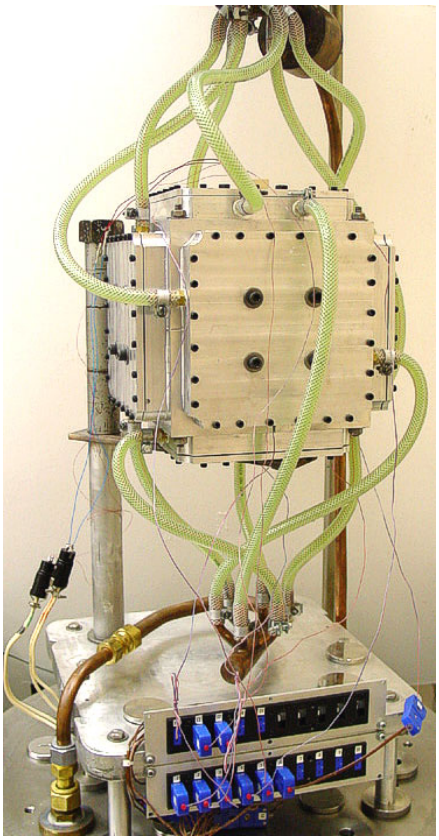

Figure 6. ENCLOSURE TEST APPARATUS IN VACUUM CHAMBER

3. Measure transient temperature data during cooling test to form empirical correlation of radiation heat transfer as a function of temperature
4. Perform transient convection measurements, starting at atmospheric conditions, to determine Q_{tot} and Q from Eq. (10)
5. Reduce air pressure in chamber and repeat convection measurements, such that at least two tests are performed per decade of Rayleigh number and the data overlap
6. Continue reducing pressure and repeating the convection tests until the diffusive limit is achieved for at least two decades of Rayleigh number.

Measurements were performed for each of the thirteen combinations presented in Fig. 7 according to the test method described above. The enclosure was maintained at a constant temperature of 22^oC and the starting and ending temperatures for the temperature difference for the transient convection tests were 50^oC and 10^oC, respectively. Data from tests performed at subsequent pressure ranges tended to overlap, and data were selected from each range that provide a smooth transition and a continuous trend over the full range of Rayleigh number. The resulting final data set for the example of the concentric cubes is plotted in terms of the dimensionless parameters $Nu_{\sqrt{A_i}}$ and $Ra_{\sqrt{A_i}}$ in Fig. 8, along with error bars which represent the accumulated

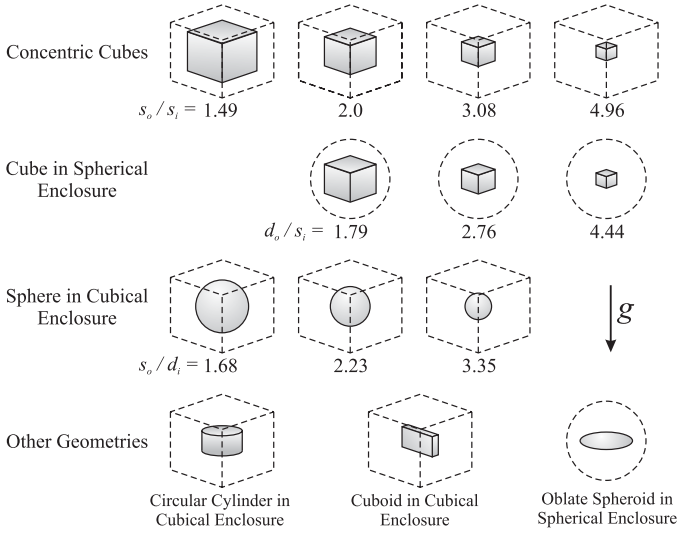

Figure 7. SUMMARY OF ENCLOSURE GEOMETRIES FOR EXPERIMENTAL TEST PROGRAM

uncertainty in the measured values. Uncertainty values for the Nusselt number varied from 2.1 to 2.3 %, while the uncertainty for the Rayleigh number was between 1.4 and 3.4 %. Data from tests for the remaining enclosure configurations will be presented during validation of the model in a subsequent section.

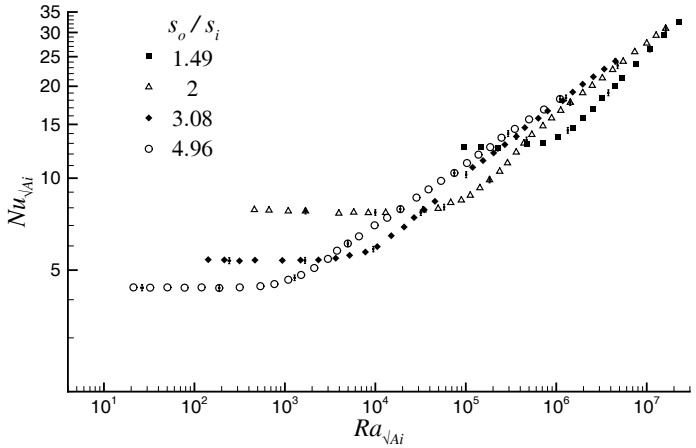

Figure 8. CONVECTION TEST RESULTS: CONCENTRIC CUBES

MODEL DEVELOPMENT

In Teertstra et al. [33] an analytical model is developed for natural convection in the concentric spherical enclosure. Unlike the previous models that are based on a combination of two terms that account for the conduction and laminar boundary layer limits, Teertstra et al. [33] present a model comprised of a combination of three asymptotic solutions. The basis of the model is the linear superposition of the convective asymptote with the diffusive limit, as recommended by Yovanovich [34] for convex isothermal bodies. Assuming that this relationship holds for the enclosure problem as well, the convective component Nu_{conv} of the total heat transfer rate measured during the experimental test program can be determined from

$$Nu_{\text{conv}} = Nu_{\sqrt{A_i}} - S^{\star}_{\sqrt{A_i}} \tag{14}$$

Convection-only experimental data, Nu_{conv}, computed using Eq. (14) for the $s_o/s_i = 2$ concentric cubical enclosure are presented in Fig. 9. This plot clearly demonstrates that, once the conduction portion of the heat transfer has been reduced from the data, the relationship between Nusselt and Rayleigh approaches a second asymptotic solution for $Ra_{\sqrt{A_i}} < 3 \times 10^5$. This third asymptote accounts for changes that occur in the transition region, where boundary layers merge, a velocity distribution is established in the core and a transition flow pattern emerges.

The general form of the three term model is

$$Nu_{\sqrt{A_i}} = S^{\star}_{\sqrt{A_i}} + \left(Nu_{\text{tr}}^{-n} + Nu_{\text{bl}}^{-n}\right)^{-1/n} \tag{15}$$

where Nu_{tr} and Nu_{bl}, the asymptotic solutions for the transition flow and laminar boundary layer flow, are combined using the Churchill and Usagi [35] composite technique.

The square root of the inner body surface area, $\sqrt{A_i}$, is selected as the characteristic length based on two criteria. First, for large aspect ratio enclosures the heat transfer is controlled by convection at the inner boundary; therefore, the scale length

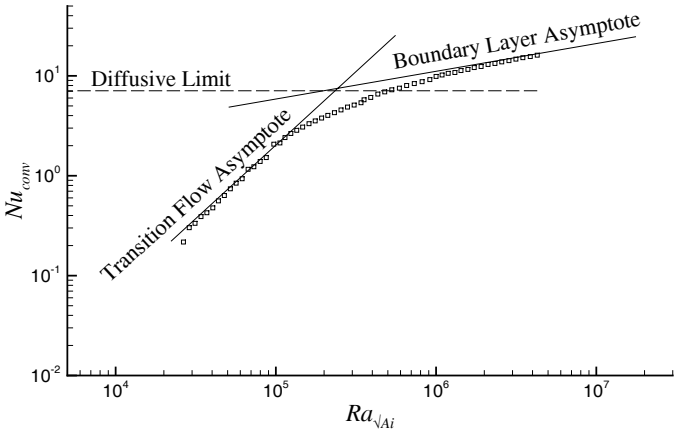

Figure 9. CONVECTION-ONLY REDUCED EXPERIMENTAL DATA: CONCENTRIC CUBES, $s_o/s_i = 2$

should be independent of the outer boundary dimensions. Second, Yovanovich [34] and Jafarpur [36] have shown that, when $\sqrt{A_i}$ is used as the scale length, equivalent bodies of similar shape and aspect ratio that are more easily characterized can be used to model complex geometries.

In the following sections, component models for each of the asymptotes in Eq. (15) developed by Teertstra et al. [33] for the concentric spheres will be expanded to include arbitrarily shaped enclosure geometries.

Conduction Shape Factor

Teertstra et al. [37] present a modeling procedure for the conduction shape factor in the region between concentric arbitrarily shaped inner and outer boundaries based on an equivalent spherical shell, where the inner and outer diameter are determined by preserving the inner surface area and enclosed volume

$$S^{\star}_{\sqrt{A_i}} = \frac{2\sqrt{\pi}}{\left[1+6\sqrt{\pi}\dfrac{V}{A_i^{3/2}}\right]^{1/3} - 1} + S^{\star}_{\infty} \tag{16}$$

where V is the total enclosed volume. Relationships for the conduction shape factor for the inner body in a full space region, $S^{\star}_{\infty}$, for all bodies considered in this work are presented by Yovanovich [38]. The model has been shown to be in excellent agreement, within 1 - 3 % RMS, with available numerical data for a variety of concentric enclosure geometries.

Laminar Boundary Layer Convection

At the limit of large Rayleigh number, the heat transfer in the enclosure is dominated by laminar boundary layer convection. Assuming the fluid in core region is of uniform temperature and the gap spacing, δ, is large compared to the boundary layer thickness, the asymptote is modeled as a series combination of convective resistances at the inner and outer boundaries. These resistance components are determined based on the models presented by Yovanovich [34] and Jafarpur [36] for natural convection from isothermal, arbitrarily shaped convex bodies

$$Nu_{\sqrt{A}} = F(Pr)\, G_{\sqrt{A}} Ra_{\sqrt{A}}^{1/4} \tag{17}$$

where the Prandtl number of function of Churchill and Churchill is

$$F(Pr) = \frac{0.67}{\left[1+(0.5/Pr)^{9/16}\right]^{4/9}} \tag{18}$$

and the body gravity function, $G_{\sqrt{A}}$, is defined by Lee et al. [39] as

$$G_{\sqrt{A}} = \left[\frac{1}{A}\iint_A \left(\frac{P\sin\theta}{\sqrt{A}}\right)^{1/3} dA\right]^{3/4} \tag{19}$$

By combining these relationships for the inner and outer boundaries, Teertstra et al. [33] present the following model for the laminar boundary layer convective asymptote for arbitrarily shaped enclosures

$$Nu_{\mathrm{bl}} = \frac{F(Pr)\, G_{\sqrt{A_i}} Ra_{\sqrt{A_i}}^{1/4}}{\left[1+\left(\dfrac{A_i}{A_o}\right)^{7/10}\left(\dfrac{G_{\sqrt{A_i}}}{G_{\sqrt{A_o}}}\right)^{4/5}\right]^{5/4}} \tag{20}$$

where differences in the shape, orientation and aspect ratio between the inner and outer boundaries are accounted for by the ratio of the body gravity functions, $G_{\sqrt{A_i}}/G_{\sqrt{A_o}}$.

Transition Flow Convection

The third asymptotic solution corresponds to the convective heat transfer that occurs in the transition between the conduction and laminar boundary layer limits. As the Rayleigh number decreases the boundary layers on the inner and outer surfaces grow and eventually merge along the midplane when $Ra < Ra_{cr}$. For Rayleigh number near the critical value, most of the heat transfer occurs by conduction in the central region, as shown in Fig. 10. The temperature distribution in the fluid gap results in a small buoyancy induced flow with the region, directed upwards in the inner half and downwards in the outer half. At the limit of small

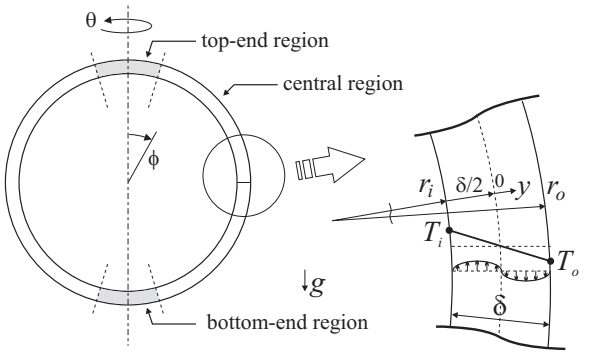

Figure 10. TRANSITION FLOW IN EQUIVALENT SPHERICAL ENCLOSURE

gap spacing, $\delta \ll \sqrt{A_i}, \sqrt{A_o}$, the problem becomes equivalent to the flow field established between vertical, differentially heated parallel plates. Based on a solution of the momentum and energy equations for this simplified geometry the effective temperature and velocity distributions in the core region are determined. The flow and temperature distribution in the central region results in an enthalpy flux to and from the upper and lower regions shown in Fig. 10, resulting in convective heat transfer in these regions.

Based on the analysis of Teertstra et al. [33] for the concentric spherical enclosure, and assuming that the transition flow for arbitrarily-shaped enclosure can be modeled using an equivalent spherical enclosure, the following expression is developed for the transition flow asymptote

$$Nu_{\rm tr} = \frac{\pi}{2880}\frac{\sqrt{A_i}}{L'}\left(\frac{\delta_e}{\sqrt{A_i}}\right)^3 Ra_{\sqrt{A_i}} \tag{21}$$

where δ_e is the effective gap spacing and L' is the effective length of the equivalent cavity. In the case of an arbitrarily shaped enclosure, the effective gap spacing is determined by the same equivalent spherical shell approximations used in the conduction shape factor model. Preserving the surface area of the interior body and the enclosed volume yields

$$\frac{\delta_e}{\sqrt{A_i}} = \frac{1}{2\sqrt{\pi}}\left[\left(6\sqrt{\pi}\frac{V}{A_i^{3/2}}+1\right)^{1/3}-1\right] \tag{22}$$

The effective length of the equivalent cavity, L', is determined based on an arithmetic average of the inner and outer effective lengths, $L' = (L_o + L_i)/2$, where the effective lengths L_o and L_i reflect the dimensions and shapes of the boundaries. Defining width W_{UB} as corresponding to the maximum perimeter of the body on a plane perpendicular to g provides an upper bound for the Nusselt number. For the example of a cubical boundary, the upper bound on the effective length is

$$W_{UB} = 4s, \;\; L_{UB} = \frac{A}{W_{UB}} = \frac{6s^2}{4s} = 1.5\,s \tag{23}$$

The lower bound results from defining the effective length as the minimum distance from the bottom to top stagnation points, or half the minimum perimeter of the body on a plane parallel to the gravity vector. For the cube, the lower bound is

$$L_{LB} = 2\,s \tag{24}$$

The bounds on the effective lengths for both the inner and outer surfaces are combined using a geometric mean

$$L' = \frac{1}{2}\sqrt{(L_o+L_i)_{UB}\,(L_o+L_i)_{LB}} \tag{25}$$

Model Summary

The three term model for natural convection in enclosures with arbitrarily shaped inner and outer boundaries is summarized as follows:

$$Nu_{\sqrt{A_i}} = S^{\star}_{\sqrt{A_i}} + \left(Nu_{\rm tr}^{-2} + Nu_{\rm bl}^{-2}\right)^{-1/2} \tag{26}$$

$$S^{\star}_{\sqrt{A_i}} = \frac{2\sqrt{\pi}}{\left[1+6\sqrt{\pi}\dfrac{V}{A_i^{3/2}}\right]^{1/3}-1} + S^{\star}_{\infty} \tag{27}$$

$$Nu_{\rm bl} = \frac{F(Pr)\,G_{\sqrt{A_i}}Ra^{1/4}_{\sqrt{A_i}}}{\left[1+\left(\dfrac{A_i}{A_o}\right)^{7/10}\left(\dfrac{G_{\sqrt{A_i}}}{G_{\sqrt{A_o}}}\right)^{4/5}\right]^{5/4}} \tag{28}$$

$$Nu_{\rm tr} = \frac{\pi}{2880}\frac{\sqrt{A_i}}{L'}\left(\frac{\delta_e}{\sqrt{A_i}}\right)^3 Ra_{\sqrt{A_i}} \tag{29}$$

$$\frac{\delta_e}{\sqrt{A_i}} = \frac{1}{2\sqrt{\pi}}\left[\left(6\sqrt{\pi}\frac{V}{A_i^{3/2}}+1\right)^{1/3}-1\right] \tag{30}$$

where a combination parameter value $n = 2$ is selected for the composite solution that provides a good fit of the experimental data.

MODEL APPLICATION

The general modeling procedure described in the previous section and summarized in Eqs. (26 - 30) is applied to the six different enclosure geometries examined in the experimental test program in the following section. In each case, formulations are

Table 1. BODY GRAVITY FUNCTION VALUES

Body	$G_{\sqrt{A}}$
Sphere	1.014
Cube	0.985
Circular Cylinder $(d/H = 2)$	0.974
Oblate Spheroid $(b/c = 3.31)$	0.873
Cuboid $(s_3/s_1 = 3.785, s_2/s_1 = 2.175)$	1.059

presented for the conduction shape factor and the transition flow asymptote. Body gravity function values are calculated using relationships for cuboids, spheroids and other geometries presented by Yovanovich and Jafarpur [40] and Lee et al. [39], as presented in Table 1. It is left to the reader to derive the more straightforward quantities, such as surface area and enclosed volume.

Concentric Cubical Enclosure

$$S^{\star}_{\sqrt{A_i}} = \frac{2\sqrt{\pi}}{\left(1+\frac{\sqrt{\pi}}{\sqrt{6}}\left[\left(\frac{s_o}{s_i}\right)^3-1\right]\right)^{1/3}-1}+3.391 \qquad (31)$$

$$Nu_{\rm tr} = \frac{\sqrt{2/\pi}}{11520}\frac{\left[\left(\frac{\sqrt{\pi}}{\sqrt{6}}\left[\left(\frac{s_o}{s_i}\right)^3-1\right]+1\right)^{1/3}-1\right]^3}{\left(1+\frac{s_o}{s_i}\right)} Ra_{\sqrt{A_i}} \qquad (32)$$

Sphere in Cubical Enclosure

$$S^{\star}_{\sqrt{A_i}} = \frac{2\sqrt{\pi}}{\left[(6/\pi)^{1/3}\, s_o/d_i - 1\right]} + 2\sqrt{\pi} \qquad (33)$$

$$Nu_{\rm tr} = \frac{\sqrt{2/\pi}}{11520}\frac{\left[\left(\frac{6}{\pi}\left[\left(\frac{s_o}{d_i}\right)^3-\frac{\pi}{6}\right]+1\right)^{1/3}-1\right]^3}{\sqrt{\left(1+\frac{3}{2}\,\frac{s_o}{d_i}\right)\left(1+\frac{4}{\pi}\,\frac{s_o}{d_i}\right)}} Ra_{\sqrt{A_i}} \qquad (34)$$

Cube in Spherical Enclosure

$$S^{\star}_{\sqrt{A_i}} = \frac{2\sqrt{\pi}}{\left(1+\frac{\pi\sqrt{\pi}}{6\sqrt{6}}\left[\left(\frac{d_o}{s_i}\right)^3-\frac{6}{\pi}\right]\right)^{1/3}-1}+3.391 \qquad (35)$$

$$Nu_{\rm tr} = \frac{\sqrt{2/\pi}}{12288}\frac{\left[\left(\frac{\pi\sqrt{\pi}}{6\sqrt{6}}\left[\left(\frac{d_o}{s_i}\right)^3-\frac{6}{\pi}\right]+1\right)^{1/3}-1\right]^3}{\sqrt{\left(1+\frac{2}{3}\,\frac{d_o}{s_i}\right)\left(1+\frac{\pi}{4}\,\frac{d_o}{s_i}\right)}} Ra_{\sqrt{A_i}} \qquad (36)$$

Circular Cylinder in Cubical Enclosure

$$S^{\star}_{\sqrt{A_i}} = \frac{2\sqrt{\pi}}{\left(1+\frac{6\sqrt{2}}{\sqrt{\pi}}\frac{\left[\left(\frac{s_o}{d_i}\right)^3-\frac{\pi}{4}\frac{H_i}{d_i}\right]}{\left(\frac{2H_i}{d_i}+1\right)^{3/2}}\right)^{1/3}-1}+3.414 \qquad (37)$$

$$Nu_{\rm tr} = \frac{\frac{1}{\sqrt{1+\frac{H_i}{d_i}}}\left[\left(\frac{6}{\pi}\frac{\left[\left(\frac{s_o}{d_i}\right)^3-\frac{\pi}{4}\frac{H_i}{d_i}\right]}{\left(\frac{1}{2}+\frac{H_i}{d_i}\right)^{3/2}}+1\right)^{1/3}-1\right]^3}{11520\sqrt{\left[1+\frac{3}{2}\,\frac{s_o/d_i}{\left(\frac{1}{2}+\frac{H_i}{d_i}\right)}\right]\left[1+\frac{2\,s_o/d_i}{\left(1+\frac{H_i}{d_i}\right)}\right]}} Ra_{\sqrt{A_i}} \qquad (38)$$

Cuboid in Cubical Enclosure

$$S^{\star}_{\sqrt{A_i}} = \frac{2\sqrt{\pi}}{\left(1+\frac{\frac{6\sqrt{\pi}}{\sqrt{2}}\left(\frac{s_o^3}{s_1\,s_2\,s_3}-1\right)}{\left[(s_1\,s_2\,s_3)^{1/3}\left(\frac{1}{s_1}+\frac{1}{s_2}+\frac{1}{s_3}\right)\right]^{3/2}}\right)^{1/3}-1}+3.469 \qquad (39)$$

$$Nu_{\rm tr} = \frac{\sqrt{2/\pi}}{12288} \frac{\sqrt{\dfrac{\left(1+\dfrac{s_3}{s_1}\right)}{\left(1+\dfrac{s_2}{s_1}\right)}} \left[\left(\dfrac{3\sqrt{\pi}}{\sqrt{2}} \dfrac{\left[\left(\dfrac{s_o}{s_1}\right)^3 - \dfrac{s_2}{s_1}\dfrac{s_3}{s_1} \right]}{\left[\dfrac{s_2}{s_1}\left(1+\dfrac{s_3}{s_1}\right) + \dfrac{s_3}{s_1} \right]^{3/2}} + 1 \right)^{1/3} - 1 \right]^3}{\sqrt{\left[1 + \dfrac{3}{2}\dfrac{s_o}{s_1} \dfrac{\left(1+\dfrac{s_3}{s_1}\right)}{\left[\dfrac{s_2}{s_1}\left(1+\dfrac{s_3}{s_1}\right) + \dfrac{s_3}{s_1} \right]} \right] \left[1 + \dfrac{2s_o}{s_1} \dfrac{1}{\left(1+\dfrac{s_2}{s_1}\right)} \right]}} Ra_{\sqrt{A_i}} \tag{40}$$

Oblate Spheroid in Spherical Enclosure

$$S^*_{\sqrt{A_i}} = \frac{2\sqrt{\pi}}{\left(1 + 6\sqrt{\pi} \dfrac{\left[\dfrac{\pi}{6}\left(\dfrac{d_o}{b_i}\right)^3 - \dfrac{4\pi}{3}\dfrac{c_i}{b_i} \right]}{\left[2\pi + \dfrac{\pi}{\varepsilon_i}\left(\dfrac{c_i}{b_i}\right)^2 \ln\left(\dfrac{1+\varepsilon_i}{1-\varepsilon_i}\right) \right]^{3/2}} \right)^{1/3} - 1} + 3.483 \ , \qquad \varepsilon_i = \sqrt{1-\left(\frac{c_i}{b_i}\right)^2} \tag{41}$$

$$Nu_{\rm tr} = \frac{\dfrac{1}{5760\sqrt{\pi}}}{\sqrt{3\left(1+\dfrac{c_i}{b_i}\right) - \sqrt{\left(1+\dfrac{3c_i}{b_i}\right)\left(3+\dfrac{c_i}{b_i}\right)}}} \left[\left(\dfrac{\left[\left(\dfrac{d_o}{b_i}\right)^3 - \dfrac{8c_i}{b_i} \right]}{\left[2 + \dfrac{1}{\varepsilon_i}\left(\dfrac{c_i}{b_i}\right)^2 \ln\left(\dfrac{1+\varepsilon_i}{1-\varepsilon_i}\right) \right]^{3/2}} + 1 \right)^{1/3} - 1 \right] Ra_{\sqrt{A_i}}}{\sqrt{\left(1 + \dfrac{2d_o/b_i}{\left[2 + \dfrac{1}{\varepsilon_i}\left(\dfrac{c_i}{b_i}\right)^2 \ln\left(\dfrac{1+\varepsilon_i}{1-\varepsilon_i}\right) \right]} \right) \left(1 + \dfrac{d_o/b_i}{\left[3\left(1+\dfrac{c_i}{b_i}\right) - \sqrt{\left(1+\dfrac{3c_i}{b_i}\right)\left(3+\dfrac{c_i}{b_i}\right)} \right]} \right)}} \tag{42}$$

MODEL VALIDATION

The general modeling procedure developed in the previous section and applied to the six particular geometries of interest in the study in Table 1 and Eqs. (31 - 42) is validated using data from the experimental test program. RMS and maximum percent differences between the data and the model for each configuration are presented in Table 2.

The model predictions for the concentric cubical enclosure for $s_o/s_i = 1.49, 2.0, 3.08$ and 4.96 are compared with the experimental data in Fig. 11. This plot shows the excellent agreement between the data and the model over most values of $Ra_{\sqrt{A}}$ and s_o/s_i, with an RMS difference of 2 - 4 % and a maximum difference of 5 - 9 %. The largest differences occur at intermediate values of Rayleigh number when $s_o/s_i = 1.49$, where the limitations of the effective gap spacing model based on an equivalent spherical shell used in the transition flow asymptote become apparent.

Figures 12 and 13 compare the models and data for the sphere in a cubical enclosure and the cube in a spherical enclosure for the six different cases examined during the experiments.

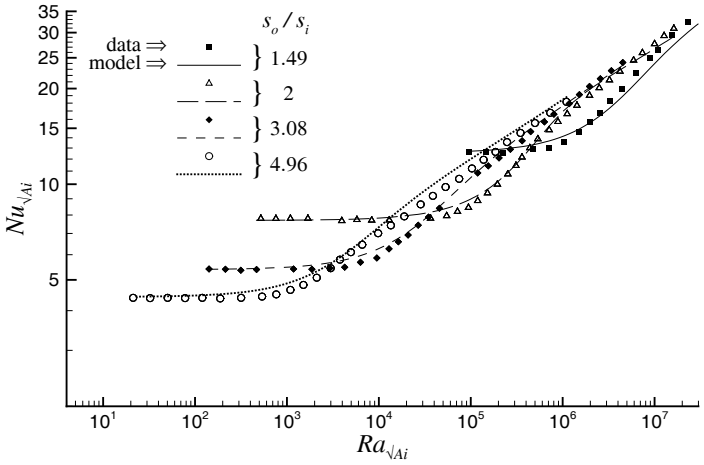

Figure 11. MODEL VALIDATION: CONCENTRIC CUBES

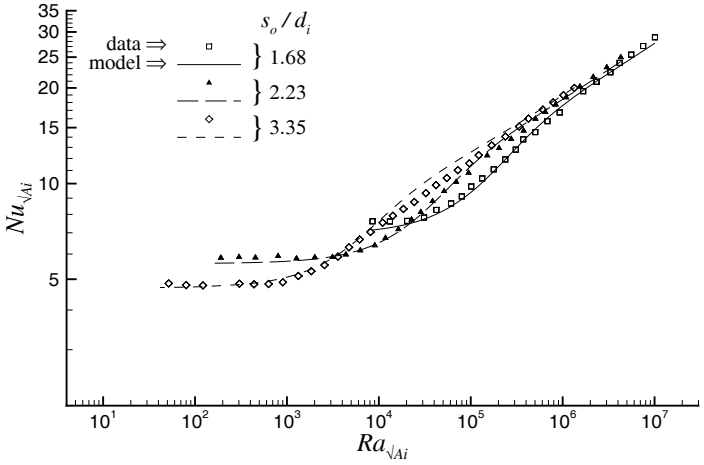

Figure 12. MODEL VALIDATION: SPHERE IN CUBICAL ENCLOSURE

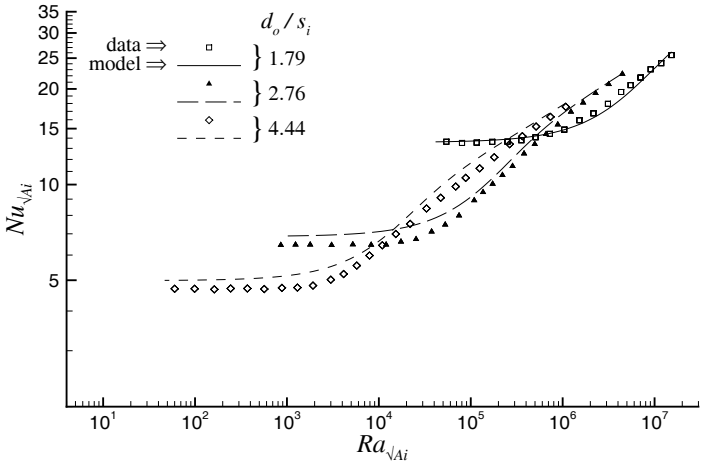

Figure 13. MODEL VALIDATION: CUBE IN SPHERICAL ENCLOSURE

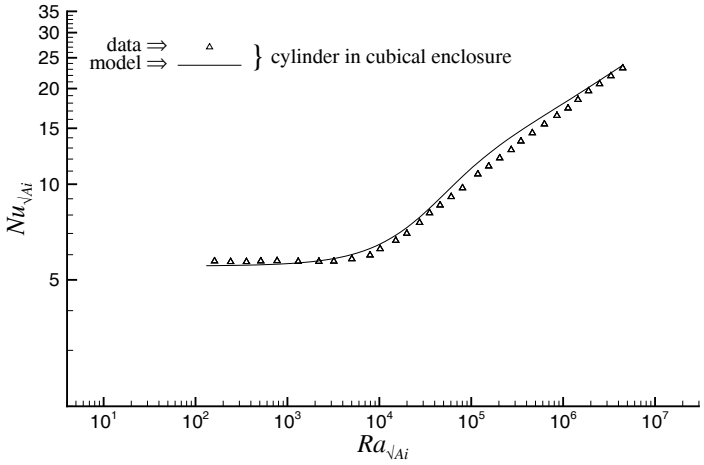

Figure 14. MODEL VALIDATION: CYLINDER IN CUBICAL ENCLOSURE

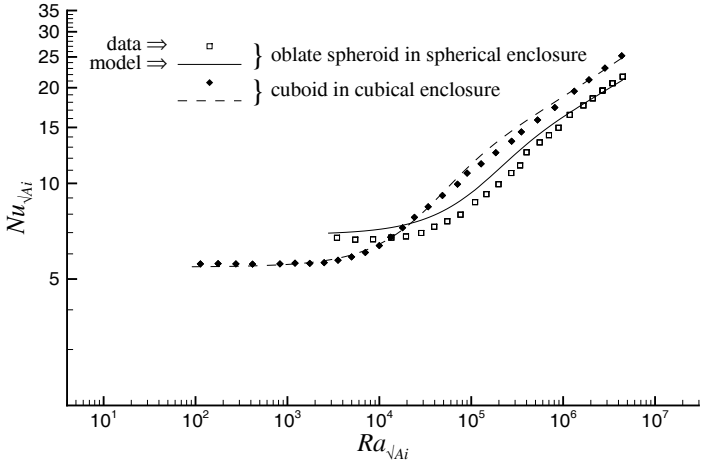

Figure 15. MODEL VALIDATION: OTHER ENCLOSURE GEOMETRIES

In both cases, the convective portion of the model provides an excellent fit of the heat transfer data at large $Ra_{\sqrt{A_i}}$, with an RMS difference in both cases of 2 - 7 %. The largest difference in both cases occurs at the diffusive limit, where inaccuracies result from the inability of the current effective gap spacing model to capture the effects of variations in the local gap thickness.

The models for the cylinder and cuboid in a cubical enclosure and the oblate spheroid in a spherical enclosure are compared with the experimental data in Figs. 14 and 15. As in the previous cases, the is very good agreement between the data and the model predictions, with an RMS difference of 3 - 7 % for all three configurations. The largest difference occurs for the oblate spheroid-in-sphere case at intermediate values of Rayleigh number, where the use of the equivalent spherical shell to predict the effective gap spacing in the transition flow asymptote results in an overprediction of $Nu_{\sqrt{A_i}}$ of approximately 12 %.

Table 2. COMPARISON OF MODEL PREDICTIONS VERSUS DATA

Enclosure	Dimensions	*RMS %*	*max. %*
Concentric Cubes	$s_o/s_i = 1.49$	4.7	7.7
	2	3.1	5.7
	3.08	2.6	6.4
	4.96	5.3	9.2
Cube in Sphere	$d_o/s_i = 1.79$	2.4	5.5
	2.76	7.2	11.1
	4.44	7.3	11.2
Sphere in Cube	$s_o/d_i = 1.68$	2.3	6.2
	2.23	2.5	5.1
	3.35	4.6	8.9
Oblate Spheroid in Spherical Enclosure		7.8	11.9
Cylinder in Cubical Enclosure		5.6	9.9
Cuboid in Cubical Enclosure		3.2	7.7

In general, the three term model is in very good agreement with the data from the experimental test program for all enclosure configurations examined in this work. The model accurately reflects all aspects of the physical behavior of the system, including the transition from conduction to convection dominated heat transfer, as well as the effects of substantial changes to the relative size and shape of the inner and outer boundaries.

SUMMARY

A combined experimental and analytical investigation of natural convection heat transfer in the three dimensional region formed between arbitrarily shaped, non intersecting isothermal boundaries has been presented. Experiments were performed for thirteen different geometries, including the concentric cubes as well as enclosures formed between different boundary shapes, such spheres, cubes and other bodies. By performing the measurements in a vacuum chamber using the transient test method, data were collected for the full range of Rayleigh number from laminar boundary layer convection at atmospheric conditions to conduction dominated heat transfer in a reduced pressure environment. An uncertainty analysis was performed on all instrumentation and measurement techniques, resulting in uncertainties of $\pm$ 1.4 to 3.4 % for the Rayleigh number and $\pm$ 2.1 to 2.3 % for the Nusselt number.

A modeling procedure is presented for the average heat transfer rate due to natural convection in the enclosure, applicable to a wide variety of shapes, sizes and orientations of both the inner and outer boundaries. The model is valid for the full range of Rayleigh number from the diffusive limit through the transition region to the laminar boundary layer limit. No empirically derived coefficients are required as input to the model, and the combination parameter used in the composite solution, $n = 2$, is a constant value that does not change for all geometries examined in this work. For the concentric cubical enclosure, the RMS difference between the data and the model is 2 - 5 %, while for all enclosures formed by combining dissimilar boundary shapes the RMS difference is between 2 and 6 %. The maximum difference between the data and model of 12 % occurs for the oblate spheroid in a spherical enclosure.

ACKNOWLEDGMENT

The authors acknowledge Materials and Manufacturing Ontario (MMO), the Natural Sciences and Engineering Research Council of Canada (NSERC) and the Centre for Microelectronics Assembly and Packaging (CMAP) for their continued financial support of this research.

REFERENCES

[1] Bishop, E.H., Kolflat, R.S., Mack, L.R. and Scanlan, J.A., 1964, "Convective Heat Transfer Between Concentric Spheres," *Proceedings of the 1964 Heat Transfer and Fluid Mechanics Institute,* Stanford University Press, Stanford, CA, pp. 69 - 80.

[2] Bishop, E. H., Mack, L. R. and Scanlan, J. A., 1966, "Heat Transfer by Natural Convection Between Concentric Spheres," *International Journal of Heat and Mass Transfer,* Vol. 9, pp. 649 - 662.

[3] Mack, L.R. and Hardee, H.C., 1968, "Natural Convection between Concentric Spheres at Low Rayleigh Numbers," *International Journal of Heat and Mass Transfer,* Vol. 11, pp. 387 - 396.

[4] Scanlan, J. A., Bishop, E. H. and Powe, R. E., 1970, "Natural Convection Heat Transfer Between Concentric Spheres," *International Journal of Heat and Mass Transfer,* Vol. 13, pp. 1857 - 1872.

[5] McCoy, C.T., Powe, R.E., Scanlan, J.A. and Bishop, E.H., 1974, "Free Convection between a Vertical Cylinder and a Spherical Enclosure," *Proceedings of the 5th International Heat Transfer Conference,* Vol. 3, pp. 105 - 109.

[6] Powe, R.E., Baughman, R.C., Scanlan, J.A. and Teng, J.T., 1975, "Free Convection Flow Patterns between a Body and its Spherical Enclosure," *Journal of Heat Transfer,* Vol. 97, pp. 296 - 298.

[7] Powe, R.E., Warrington, R.O. and Scanlan, J.A., 1980, "Natural Convection Flow between a Body and Its Spherical Enclosure," *International Journal of Heat and Mass Transfer,* Vol. 23, pp. 1337 - 1350.

[8] Charmchi, M. and Sparrow, E.M., 1982, "Analysis of Natural Convection in the Space between Concentric Vertical Cylinders of Different Height and Diameter," *Numerical Heat Transfer,* Vol. 5, pp. 119 - 144.

[9] Sparrow, E.M. and Charmchi, E., 1983, "Natural Convection Experiments in an Enclosure between Eccentric or Concentric Vertical Cylinders of Different Height and Diameter," *International Journal of Heat and Mass Transfer,* Vol. 26, pp. 133 - 143.

[10] Powe, R.E. and Warrington, R.O., 1983, "Natural Convection Heat Transfer between Bodies and Their Spherical Enclosure," *Journal of Heat Transfer,* Vol. 105, pp. 440 - 446.

[11] Warrington, R.O. and Powe, R.E., 1985, "The Transfer of Heat by Natural Convection Between Bodies and their Enclosures," *International Journal of Heat and Mass Transfer,* Vol. 28, pp. 319 - 330.

[12] Warrington, R.O., Powe, R.E. and Mussulman, R.L., 1982, "Steady Conduction in Three-Dimensional Shell," *Journal of Heat Transfer,* Vol. 104, pp. 393 - 394.

[13] Warrington, R.O., Brown, P.K. and Powe, R.E., 1986, "Natural Convection Heat Transfer Within Enclosures at Reduced Pressures," *Heat Transfer 1986: Proceedings of Eighth International Heat Transfer Conference,* San Francisco, CA, Vol. 4, pp. 1483 - 1488.

[14] Teertstra, P., Yovanovich, M.M. and Culham, J.R., 2002, "Natural Convection Measurements for a Concentric Spherical Enclosure," 2002 IMECE Conference, November 17, New Orleans, LA.

[15] Astill, K.N., Leong, H. and Martorana, R., 1980, "A Numerical Solution for Natural Convection in Concentric Spherical Annuli," *Natural Convection In Enclosures,* ASME-HTD Vol. 8, pp. 105 - 113.

[16] Caltagirone, J.-P., Combarnous, M. and Mojtabi, A., 1980, "Natural Convection between Two Concentric Spheres: Transition toward a Multicellular Flow," *Numerical Heat Transfer,* Vol. 3, pp. 107 - 114.

[17] Singh, S.H. and Chen, J., 1980, "Numerical Solution for Free Convection between Concentric Spheres at Moderate Grashof Numbers," *Numerical Heat Transfer,* Vol. 3, pp. 441 - 459.

[18] Ingham, D.B., 1981, "Heat Transfer by Natural Convection between Spheres and Cylinders," *Numerical Heat Transfer,* Vol. 4, pp. 53 - 67.

[19] Wright, J.L. and Douglass, R.W., 1986, "Natural Convection in Narrow-gap, Spherical Annuli," *International Journal of Heat and Mass Transfer,* Vol. 29, No. 5, pp. 725-739.

[20] Fujii, M., Takamatsu, H. and Fujii, T., 1987, "A Numerical Analysis of Free Convection around an Isothermal Sphere (Effects of Space and Prandtl Number)," *Proceedings of the 1987 ASME/JSME Thermal Engineering Joint Conference,* Vol. 4, pp. 55 - 60.

[21] Garg, V.K., 1992, "Natural Convection between Concentric Spheres," *International Journal of Heat and Mass Transfer,* Vol. 35, pp. 1935 - 1945.

[22] Chu, H-S. and Lee, T-S., 1993, "Transient Natural Convection Heat Transfer between Concentric Spheres," *International Journal of Heat and Mass Transfer,* Vol. 36, pp. 3159 - 3170.

[23] Chiu, C.P. and Chen, W.R., 1996, "Transient Natural Convection Heat Transfer between Concentric and Vertically Eccentric Spheres," *International Journal of Heat and Mass Transfer,* Vol. 39, pp. 1439 - 1452.

[24] Raithby, G.D. and Hollands, K.G.T., 1975, "A General Method of Obtaining Approximate Solutions to Laminar and Turbulent Free Convection Problems,"*Advances in Heat Transfer,*Editors T.F. Irvine Jr. and J.P. Hartnett, Academic Press, New York, Vol. 11, pp. 265 - 315.

[25] Raithby, G.D. and Hollands, K.G.T., 1998, "Natural Convection," *Handbook of Heat Transfer,* 4th ed., eds. W.M. Rohsenow, J.P Hartnett and Y. Cho, McGraw Hill, NY, Chapter 4, 1998.

[26] Weber, N., Powe, R. E., Bishop, E. H. and Scanlan, J. A., 1973, "Heat Transfer by Natural Convection Between Vertically Eccentric Spheres," *Transactions of the ASME: Journal of Heat Transfer,* Vol. 95, pp. 47 - 52.

[27] Yin, S.H., Powe, R.E., Scanlan, J.A. and Bishop, E.H., 1973, "Natural Convection Flow Patterns in Spherical Annuli," *International Journal of Heat and Mass Transfer,* Vol. 16, pp. 1785 - 1795.

[28] Lienhard, J.H., 1973, "On the Commonality of Equations for Natural Convection from Immersed Bodies," *International Journal of Heat and Mass Transfer,* Vol. 16, pp. 2121 - 2123.

[29] Teertstra, P., 2003, "Models And Experiments For Laminar Natural Convection From Heated Bodies In Enclosures," Ph.D. Thesis, Department of Mechanical Engineering, University of Waterloo, Waterloo, Ontario, Canada.

[30] Chamberlain, M.J., Hollands, K.G.T. and Raithby, G.D., 1985, "Experiments and Theory on Natural Convection Heat Transfer From Bodies of Complex Shape," *Journal of Heat Transfer, Transactions ASME,* Vol. 107, pp. 624 - 629.

[31] Hassani, A.V. and Hollands, K.G.T, 1989, "On Natural Convection Heat Transfer From Three-Dimensional Bodies of Arbitrary Shape," *Journal of Heat Transfer, Transactions ASME,* Vol. 111, pp. 363 - 371.

[32] Hollands, K. G. T., 1988, "Direct Measurement of Gaseous Natural Convection Heat Fluxes," *Proc. First World Conf. Exp. Heat Transfer, Fluid Mechanics and Thermodynamics,* eds. R. K. Shah, E. N. Ganic and K. T. Yang, pp. 160 - 168.

[33] Teertstra, P., Yovanovich, M.M. and Culham, J.R., 2004, "Analytical Modeling of Natural Convection in Concentric Spherical Enclosures," AIAA-2004-0496, *42nd AIAA Aerospace Sciences Meeting and Exhibit,* Reno, NV, Jan. 5 - 8.

[34] Yovanovich, M.M., 1987, "New Nusselt and Sherwood Numbers for Arbitrary Isopotential Geometries at Near Zero Peclet and Rayleigh Numbers," *AIAA 22nd Thermophysics Conference,* AIAA-87-1643.

[35] Churchill, S.W. and Usagi, R., 1972, "A General Expres-

sion for the Correlation of Rates of Transfer and Other Phenomenon," *American Institute of Chemical Engineers Journal,* Vol. 18, pp. 1121 - 1128.

[36] Jafarpur, K., 1992, "Analytical and Experimental Study of Laminar Free Convective Heat Transfer from Isothermal Convex Bodies of Arbitrary Shape," Ph.D. Thesis, Department of Mechanical Engineering, University of Waterloo, Waterloo, Ontario, Canada.

[37] Teertstra, P., Yovanovich, M.M. and Culham, J.R., 2003, "Conduction Shape Factor Models for 3-D Enclosures," AIAA-2003-0159, *41st AIAA Aerospace Sciences Meeting and Exhibit,* Reno, NV, Jan. 6.

[38] Yovanovich, M. M., 1998, "Conduction and Thermal Contact Resistances (Conductances)," *Handbook of Heat Transfer,* 3rd. ed., eds. W. M. Rohsenow, J. P. Harnett and Y. Cho, McGraw Hill, New York, Chapter 3, pp. 3.1 - 3.73.

[39] Lee, S., Yovanovich, M. M. and Jafarpur, K., 1991, "Effects of Geometry and Orientation on Laminar Natural Convection Heat Transfer from Isothermal Bodies," *Journal of Thermophysics and Heat Transfer,* Vol. 5, pp. 208 - 216.

[40] Yovanovich, M.M. and Jafarpur, K., 1993, "Models of Laminar Natural Convection from Vertical and Horizontal Isothermal Cuboids for all Prandtl Numbers and All Rayleigh Numbers Below 10^{11}," *Fundamentals of Natural Convection,* ASME HTD Vol. 264, pp. 111 - 126.